PREPARATION AND PROPERTIES OF PALLADIUM AND PLATINUM SUPPORTED ON LAYER SILICATE MINERALS

BY

JEFFREY BAKER HARRISON

A DISSERTATION PRESENTED TO THE GRADUATE COUNCIL
OF THE UNIVERSITY OF FLORIDA IN
PARTIAL FULFILLMENT OF THE REQUIREMENTS
FOR THE DEGREE OF DOCTOR OF PHILOSOPHY

UNIVERSITY OF FLORIDA

1982

Ad Majorem Dei Gloriam

Annuit Coeptis

ACKNOWLEDGEMENTS

The last five years I have spent studying at the University of Florida and living in Gainesville have been, perhaps, the most formative and influential of my life. I have experienced success and failure, but more importantly I have grown in intellect and maturity as a result of my research experience and my interactions with the people of this community. Particularly notable in this regard, is the relationship I developed with my major professor Dr. Vaughn E. Berkheiser. He has served as my teacher, my counselor, and especially my friend. To him I owe a special debt of gratitude. Also particularly worthy of mention are the other members of my committee, Dr. B.G. Volk, Dr. J.J. Street, and Dr. W.S. Brey, whose advice and guidance have made my years at the University a pleasant and rewarding experience. To my loving parents I give all my appreciation for their moral and financial support which they always provided without question. Although a brief mention here can hardly serve as repayment for all the work and services performed, this list would not be complete without mention of Rudy Strohschein, Jr.--a very talented glassblower.

Finally, I would like to acknowledge my son Eliot, whose unvacillating love has given me purpose, strength, and understanding even in the most troubling of times.

TABLE OF CONTENTS

	Page
ACKNOWLEDGEMENTS	iii
ABSTRACT	vi
CHAPTER I: HYDROGEN REDUCTION OF $Pt(NH_3)_4^{2+}$ SUPPORTED ON MONTMORILLONITE	1
Introduction	1
Experimental	4
Results	7
Infrared Analysis	7
Stoichiometry of Reduction	9
X-ray Analysis	9
Transmission Electron Microscopy (TEM)	11
Discussion	12
Conclusions	17
CHAPTER II: HYDROGEN REDUCTION OF $Pd(NH_3)_4^{2+}$ SUPPORTED ON MONTMORILLONITE	25
Introduction	25
Experimental	26
Results	28
Infrared Spectroscopy	28
X-ray Analysis	30
Transmission Electron Microscopy (TEM)	31
Discussion	33
Conclusions	37
CHAPTER III: MOLECULAR HYDROGEN INTERACTION WITH LAYER SILICATE SUPPORTED Pd AND Pt CATALYSTS	46
Introduction	46
Experimental	48
Results	49
Discussion	52
Conclusions	56

Page

CHAPTER IV: CONDENSED PHASE HYDROGENATION OF 1-HEXENE BY Pd AND Pt MONTMORILLONITE SUPPORTED CATALYSTS. 65

Introduction 65

Experimental 67

Results. 68

Discussion 70

Conclusions. 72

REFERENCES. 75

BIOGRAPHICAL SKETCH 78

Abstract of Dissertation Presented to the Graduate Council of the University of Florida in Partial Fulfillment of the Requirements for the Degree of Doctor of Philosophy

PREPARATION AND PROPERTIES OF PALLADIUM AND PLATINUM SUPPORTED ON LAYER SILICATE MINERALS

By

Jeffrey Baker Harrison

May 1982

Chairman: Bob G. Volk
Cochairman: Vaughn E. Berkheiser
Major Department: Soil Science

The addition of molecular hydrogen at 140°C to $Pd(NH_3)_4^{2+}$ and $Pt(NH_3)_4^{2+}$ complexes exchanged on Wyoming montmorillonites, at various metal weight to support weight ratios, results in metal reduction according to the mechanism $M(NH_3)_4^{2+} + H_2 \rightarrow M^\circ + 2NH_4^+ + 2NH_3$. In a parallel reaction, the concurrent reduction of structural iron (III) occurs, producing an increase in the layer charge of the mineral. Charge balance is maintained by the additional formation of ammonium cations by ammine protonation.

Metal reduction is accompanied by the collective migration of atoms and/or crystallites from the internal surface of the mineral to sites, on the external surface and edges, of low negative charge. At high metal concentrations, large clusters of >100Å are easily visible by transmission electron microscopy.

Also apparent is a high proportion of the metal crystallites formed in diameters of 50Å or less. As the metal concentration decreases, mean metal diameters decrease and the particle size distributions become narrower.

Attempts to measure metal dispersions (number of surface metal atoms/total number of metal atoms) by the hydrogen titration of oxygenated surface metal atoms result in a drastic overestimation of this value. The primary cause appears to be related to the spillover of atomic hydrogen from the metal to the support phase. Infrared evidence exists which implicates the role of structural iron, present in the montmorillonite support, as hydrogen atom acceptor sites. Molecular water, formed during the titration reaction, also appears to be involved in the process, acting as a carrier for hydrogen atoms between the metal surface and the acceptor sites.

Values, more indicative of the actual metal dispersion, are obtainable by measuring the gravimetric loss of water after the initial hydrogen titration. This technique offers a simple and convenient method for determining metal dispersion independent of hydrogen spillover.

Finally, the catalytic activity of palladium loaded montmorillonites is demonstrated for the hydrogenation of 1-hexene. The higher specific activity of these catalysts compared to a 5.0%Pd·Al_2O_3 would indicate the manifestation of hydrogen spillover once again.

CHAPTER I
HYDROGEN REDUCTION OF $Pt(NH_3)_4^{2+}$ SUPPORTED ON MONTMORILLONITE

Introduction

A wide variety of support materials have been utilized for platinum catalyzed reactions. The major role of the support is to provide a large surface area and a stable matrix for highly dispersed metals. As reflected by the vast amount of literature, the most popular supports for the noble metals are the synthetic faujasites or zeolites. Their ubiquitous use is founded on high metal dispersion upon gas phase reduction of metal cations and their apparent influence on the electronic properties of the metal.

Intrinsically, layer silicate minerals possess many of the same surface properties as zeolites; yet in comparison, they have been largely ignored as support matrices. Smectites, one class of layer lattice silicates, appear to be particularly well-suited as a support material because of their large internal surface area (100-800 m^2/g), high cation exchange capacity (120 meq/gm), and an inducable extremely high surface acidity.

A smectite mineral is composed of units of two silica tetrahedral sheets linked by oxygen apices to a central aluminum or magnesium octahedral sheet (Fig. I-1). Isomorphic

substitution of ions of lower valence for silicon in the tetrahedral sheets and/or aluminum (or magnesium) in the octahedral sheet imparts a net negative charge to the mineral, which resides primarily in the interlayer sheet. With exchangeable cations to balance charge, the structure consists of alternating layers of negatively charged sheets and interlayered cations. The unique feature of these minerals is the ease of exchange of the interlayer cations and the expansion in the c-direction of the silicate layers by water and other polar molecules. This makes the interlayer separation dependent on the saturating cation, interlayer solvent, and the charge density of the silicate sheets.

A number of studies have documented the influence of the interlamellar surface on the formation of organometallic species on clay minerals and adsorbed transition metal complexes (1-7). The absorption spectra of these complexes differ considerably from their spectra in water, but band positions were strongly dependent on the hydration level of the mineral.

In the case of copper (II) arene complexes, two distinct species were found (1). A type I complex, observed under hydrated conditions, apparently contained a planar C_6H_6 ring. When this specimen was dehydrated, a red-colored type II complex was formed consisting of "associated radical cations" produced by electron transfer from the benzene molecule to the metal cation. Although the mineral apparently enhances the formation of this complex (i.e., stabilizes the product), no reasons were given.

Berkheiser and Mortland (4) studied the oxidation-reduction reaction of copper and iron phenanthroline complexes on hectorite. They found an apparent increase in the oxidation potential of $Fe(phen)_3^{2+}$ - $Fe(phen)_3^{3+}$ couple above that observed in water. The increase was explained in terms of a possible destabilization of the oxidized form by the silicate sheet.

When $Ru(bpy)_3^{2+}$ was adsorbed on hectorite (a trioctahedral mineral with Mg^{2+} as the predominant cation in the octahedral layer) and bentonite (an aluminous dioctahedral mineral) surfaces, a high proportion of the ligand was found in the covalently hydrated form (6). The formation of this unusual complex was attributed to the high degree of dissociation of interlamellar water. This is a consequence of the fact that at monolayer coverage the water molecules are influenced by the strong electrostatic field of the exchangeable interlayer cations. As the mineral was dehydrated, the electrostatic interaction increased and hence the surface acidity.

Recently, Pinnavaia and Welty (7) demonstrated that rhodium complexes supported on hectorite had a higher activity toward 1-hexene hydrogenation in solution phase than the same complexes supported on a Dowex 50 resin or a Rh_2^{4+} homogeneous solution. They concluded that the interlamellar surface enhanced the reactivity of Rh_2^{4+} toward metal hydride formation.

Despite the current interest in the influence of clay minerals on the behavior of transition metal complexes, it is apparent that the use of clay minerals as supports for noble metal complexes and crystallites has not been investigated.

To evaluate the utility of these minerals for supported noble metal catalysis, a study was undertaken to determine the suitability of a Wyoming montmorillonite mineral as a support for various loadings of platinum. A description of the loading of the platinum tetrammine cation and its subsequent reduction to zero valency is given. In addition, the location and electronic environment of the cation before reduction and the metal after reduction are also discussed.

Experimental

The smectite mineral support was a Wyoming (Wy.) montmorillonite obtained from The Clay Minerals Repository, University of Missouri, Columbia, Missouri. The clay was washed with 1N NaOAc (pH 5.0) at 80°C to remove carbonates and treated with Na citrate-dithonite to remove free iron and aluminum oxides. The mineral was further washed five times with NH_4Cl, followed by repeated washings with deionized H_2O until chloride was undetectable with $AgNO_3$. The <2 μm fraction was separated by centrifugation. The approximate unit cell formula of NH_4^+· Wy. montmorillonite is $NH_4^+{}_{0.90}$ $(Al_{3.07}Fe^{3+}_{0.23}Fe^{2+}_{0.18}Mg^{2+}_{0.31})(Si_{7.69}Al_{0.31})O_{20}(OH)_4$ based upon the published analysis of Ref. (8).

A fully loaded platinum catalyst was prepared by washing the <2 μm fraction five times with the tetrammine nitrate salt. The excess salt was removed by washing the metal-clay suspension with deionized water a minimum of six times. The

sample was analyzed by atomic absorption for sodium to determine the amount of platinum exchanged on the clay. All other loadings of Pt were prepared by adding an appropriate volume of tetrammine salt, equilibration for 24 hours, followed by washing until salt free.

All gas reagents were obtained from Linde Corporation in the highest grade available and were used without further purification with the exception of hydrogen which was passed through a zeolite-liquid N_2 trap.

Air-dried samples were reduced by slowly heating to 140°C under vacuum (1×10^{-5} Torr) and held there for a minimum of 6 hours. Dry hydrogen was added to the system (100 Torr) and allowed to contact the sample for 6 hours. The entire system was completely evacuated and an additional 100 Torr H_2 added for 3 hours. At this point, the sample was evacuated to less than 10^{-5} Torr for 4 hours and was ready for further treatment.

For infrared analysis, self-supporting films were made by drying a dilute suspension of the noble metal loaded clay on mylar film. By this method, the clay dries with a high proportion of the basal planes of the silicate layers aligned parallel to the plane of the mylar film. A stainless steel evacuable cell fitted with KRS-5 windows permitted the recording of IR spectra in the presence of different gases. Spectra were recorded on a Perkin Elmer 567 IR spectrophotometer.

X-ray analyses were obtained on the Diano XRD-700 X-ray diffractometer using Ni filtered Cu Kα radiation. Basal

spacings, d(001), were determined on oriented samples by using at least four orders of reflection. The presence of metal crystallites was always checked by scanning over the angles expected for the 111, 200, 220, and 311 reflections of the metal. Evacuated diffractograms were obtained by transferral of the sample from the vacuum rack to a glove bag attached to the X-ray sample mount under flowing dry He.

Transmission electron micrographs were taken at magnifications ranging from 50K to 100K with a JEOL 100C electron microscope operated at 40KV. Samples were deposited on formvar coated copper grids and examined without further treatment. Average particle diameters for each loading were calculated by using surface area based weighted average:

$$\bar{d} = \frac{\Sigma n_i d_i^3}{\Sigma n_i d_i^2} \qquad \text{(Ref. 9)}$$

The stoichiometry of reduction was determined by adding H_2 to a fully exchanged $Pt(NH_3)_4^{2+}$ · Wy. montmorillonite (8.6% Pt, w/w) heated to 140°C and trapping the liberated NH_3 at 77°K. Four hours later, flowing He was passed through the trap, as it was warmed to room temperature and passed through a water trap containing a known amount of acid. The remaining acid was titrated with a standardized base to determine the amount of NH_3 liberated during reduction.

Results

Infrared Analysis

Infrared band positions and their corresponding assignments for the unreduced and reduced platinum loaded Wy. montmorillonite are given in Table I-1. The spectrum of an evacuated M^{n+}·Wy. montmorillonite is characterized by a band at 3625 cm^{-1} which has been ascribed to the stretching vibration of the structural hydroxyls situated in the octahedral layer of the smectite (Fig. I-1). Four distinct deformation modes occurred at 920, 885, 850, and 800 cm^{-1} which resulted from bridging hydroxyls associated with different combinations of cations filling the octahedral holes of the mineral. The band assignments (after Farmer (10)) for the first two combinations are given in Table I-1.

When the mineral was fully exchanged (8.6% Pt) by the $Pt(NH_3)_4^{2+}$ cation, the IR band positions associated with the mineral remained unchanged. The amine ligands contributed a doublet to IR spectrum of the unevacuated sample located at 3290 and 3220 cm^{-1}. These have been previously assigned to the asymmetric and symmetric N-H stretching vibrations, respectively (11, 12). A corresponding deformation mode was found at 1370 cm^{-1}. Upon evacuation, the amine stretching vibrations appeared as a triplet, located at 3330, 3300, and 3220 cm^{-1}, and the deformation band shifted from 1370 cm^{-1} to 1335 cm^{-1}. Unfortunately the Pt-N stretching fundamentals

were obscured by low frequency vibrations of the aluminosilicate framework.

At lower metal loadings (3.0%, 1.0%, 0.6% Pt), there were no significant changes in the IR spectrum relative to the air-dried unreduced 8.6% Pt· Wy. montmorillonite, albeit the N-H stretching vibration of the residual ammonium cation largely obscured the ammine fundamentals in the samples containing 3.0% or less metal. The position of the ligand ammine stretching vibrations was elucidated by substituting Na^+ for NH_4^+ as the residual interlayer cation. The only changes in the IR spectrum of these metal loaded samples with evacuation was the removal of the H_2O deformation mode, a narrowing of the $\nu_a(NH_3)$ and $\nu_s(NH_3)$ fundamentals, and a shift of the $\delta_s(HNH)$ from 1370 cm^{-1} to 1345 cm^{-1}.

Moderate reducing conditions (100 Torr H_2, 140°C) produced pronounced changes in the IR spectrum at all metal loadings (Table I-1). Although the four catalysts examined differed widely in platinum concentration, the IR spectrum of the fully loaded 8.6% Pt· Wy. montmorillonite reflected the majority of changes in the lower loadings when reduced. The most notable feature was the appearance of a single broad band centered at 3260 cm^{-1} and a sharp band at 1425 cm^{-1}. Missing from the spectrum were the bands associated with stretching and bending fundamentals of the ammine ligands. In addition, there were pronounced changes in the IR bands attributed to the mineral vibrations. An apparent downward shift in the ν(OH) occurred with a corresponding upward

shift (or disappearance) of the deformation mode belonging to the δ(FeAlOH) combination. An NH_4^+·montmorillonite subjected to identical conditions showed no change in its IR spectrum. Exposure of the reduced 8.6% Pt·Wy.montmorillonite to the atmosphere for 24 hours restored the hydroxyl bands to their original positions.

Reduction of 0.6%, 1.0%, and 3.0% Pt·Wy.montmorillonites showed similar shifts in the FeAlOH deformation band although this band did not completely disappear. Rather, the band was broadened and decreased in intensity. As with the 8.6% Pt·Wy.montmorillonite, exposure to the atmosphere at room temperature restored the δ(FeAlOH) hydroxyl band to its original position and intensity.

Stoichiometry of Reduction

Three separate quantitative titrations of the ammonia released upon reduction of 1.000 gm, 8.6% Pt·Wy.montmorillonite yielded an average of 0.292 mmole ± 0.02 mmole NH_3. Using a previously determined cation exchange capacity of 0.85 meq/gm, this represents only 17% of the total ammine ligand. The remaining 83% was assumed to be converted to ammonium during the reduction process.

X-ray Analysis

A fully saturated 8.6% $Pt(NH_3)_4^{2+}$·Wy.montmorillonite heated at 80°C in vacuo, exhibited a well-ordered basal spacing of 12.1Å (Table I-2). With an ideal unit cell

dimension of 9.6Å, the interlayer spacing of 2.5Å is attributed strictly to the presence of the metal ammine cation.

Lower loadings of tetrammine cation did not produce diffractograms indicative of a well ordered structure. In most cases the higher order reflections were broad often exceeding several degrees of 2θ in width. This was particularly true when the samples were evacuated at moderate temperatures (110°C, 1 x 10^{-5} Torr). In general, the basal spacing of the evacuated sample decreased with decreasing platinum content. As Table I-2 demonstrates, the 001 reflection of 0.6% Pt·Wy.montmorillonite approached the basal spacing of an NH_4^+·Wy.montmorillonite.

The addition of 100 Torr H_2 at 140°C to the 8.6% Pt sample resulted in a decrease in the basal spacing from 12.1 to 10.6Å in the absence of water vapor (Table I-2). A similar value was found for an NH_4^+·Wy.montmorillonite treated under the same conditions. Interestingly, the fourth order reflection in this diffractogram was absent.

The 8.6% Pt catalyst showed only limited swelling properties when rehydrated for 24 hours at 97% RH and 25°C, as the basal spacing increased to only 11.1 Å under these conditions whereas an identically treated NH_4^+·Wy.montmorillonite increased to 12.8Å.

The formation of metal crystallites >50Å was indicated for the 8.6% Pt catalyst by the appearance of a weak diffuse peak at 39.8°2θ representing the 111 reflection of well-crystallized platinum. No other reflections attributable to

the metal were observed at higher angles. High noise levels at more sensitive instrument settings made line broadening measurements prohibitive. The catalysts loaded at lower Pt contents exhibited a pronounced narrowing of the (001) basal reflection upon metal reduction. When thoroughly evacuated all reduced catalysts exhibited basal spacings of 10.6 Å, identical to the value observed for the 8.6% Pt·Wy.montmorillonite after reduction and evacuation. Diffraction lines associated with metal cluster formation were never observed for the 0.6%, 1.0%, and 3.0% Pt catalysts.

Transmission Electron Microscopy (TEM)

Crystallite size distributions, deduced from electron micrographs (Fig. I-2), are shown for each catalyst loading in Fig. I-3. A narrow distribution was obtained for the 0.6% Pt·Wy.montmorillonite with 95% of the particles having a diameter less than 30Å. The average crystallite size ($\bar{d}$) at this loading was 22.9Å. A small increase in platinum concentration to 1.0% Pt considerably broadened the distribution and resulted in an overall increase in crystallite dimension. The average diameter at this loading was 42.7Å with only 54% of the particles having a diameter less than 30Å. At the 3.0% Pt level, 58% of the particles examined were less than 35Å; yet the average particle diameter was 97.9Å. This is a consequence of the appearance of a small number of clusters larger than 80Å which are heavily weighed when calculating the average particle sizes. If only crystallites less than

80Å which were counted the average diameter at the 3.0% level was 42.8Å. A similar effect was observed in the 8.6% Pt·Wy. montmorillonite. The average crystallite diameter was 158.6Å, if particles over the entire distribution were counted. Of these, 56% were less than 30Å. Taking only the particles less than 80Å gave an average diameter of 57.2 Å. However, unlike the 3.0% Pt·Wy.montmorillonite, the appearance of large clusters was not infrequent. In fact, clusters as large as 300 and 400Å were not uncommon. They appeared more as bands and films than well defined clusters and probably coalesced after the initial reduction of the metal much in the same way as the uniting of two or three water drops on a smooth surface.

Discussion

Symmetry concepts of group theory as applied to infrared spectroscopy can provide valuable information about the geometrical configuration of a molecule or changes in the configuration with specific experimental treatments. Variation in the symmetry of a molecule is generally manifested in the IR spectrum as an increase or decrease in the number of bands.

From collected infrared and raman data the $Pt(NH_3)_4^{2+}$ cation has been proven to be a square planar complex belonging to the D_{4h} point group (11, 12). When discussing the ammine ligands it is convenient to describe them in terms of a 1:1 model (metal/ligand) with local symmetry C_{3v} (13). Of particular interest in this study are the A_1 symmetric

stretching vibration, the degenerate E antisymmetric stretching mode, and the symmetric A_1 deformation mode predicted for C_{3v} symmetry. These appear in the IR spectrum of the air-dry 8.6% Pt·Wy.montmorillonite as a doublet at 3290 cm^{-1} and 3220 cm^{-1} and a single band at 1370 cm^{-1}, respectively (Table I-1). Therefore, under air-dry conditions the ammine ligands of the $Pt(NH_3)_4^{2+}$ cation retained their C_{3v} symmetry within the Wy. montmorillonite interlayer. Because all four ligands are symmetry equivalent, it is believed that under air-dried conditions, the D_{4h} symmetry of the cation is preserved.

Thorough evacuation of the catalyst at 80°C effected a splitting of the degenerate antisymmetric fundamental with bands appearing at 3330, 3300, and 3220 cm^{-1}. The lifting of the degeneracy by the removal of interlayer water must reflect a reduction in ligand symmetry as the metal-ammine complex was sandwiched between the interlamellar surfaces. This can be explained in part by restricted rotation of the complex and ligands as the mineral is dehydrated.

The symmetric deformation fundamental was particularly sensitive to the hydration status of mineral. Not unexpectedly, dehydration at 80°C in vacuo shifted the bending mode to lower frequency (from 1370 cm^{-1} to 1335 cm^{-1}) indicative of decreased hydrogen bonding.

At lower platinum loading (0.6%, 1.0%, and 3.0% Pt) these effects were not nearly as distinct due to an overlap of the stretching vibration of the residual ammonium cation and a decrease in the intensity of the ligand vibrations. When the interlayer ammonium cation is replaced by the sodium

ion, the IR spectrum showed ammine stretching vibrations at frequencies similar to those found in the air-dried 8.6% Pt $(NH_3)_4^{2+}$·Wy.montmorillonite IR spectrum. Because a significant splitting of the $\nu_a(NH_3)$ vibration was not observed with evacuation, it appears that the residual interlayer cation (NH_4^+ or Na^+) prevented the complete collapse of the interlayer. This was also reflected in the decrease shift of the δ_s(HNH) with evacuation compared to the shift observed for the 8.6% Pt sample. It is concluded that interlayer water associated with the residual cations must remain partially hydrogen bonded to the ammine ligands under these conditions.

As shown in Table I-1, the addition of H_2 at 140°C produced significant changes in the IR spectrum of the 8.6% Pt·Wy.montmorillonite. Foremost, the appearance of IR bands at 3260 cm^{-1} and 1425 cm^{-1} coupled with the disappearance of the bands associated with the ammine ligand vibrations indicated the formation of the ammonium cation. An independent titration of ammonia released during reduction confirms this mechanism. However, it was noted from these results that nearly 83% of the ammine ligand was retained by the mineral as ammonium suggesting a net increase in layer charge. Rozenson and Heller-Kallai (8, 14) demonstrated the reduction of octahedral iron in a natural Wy. montmorillonite by aqueous solutions of hydrazine, sodium dithionite, and sodium sulfide at 70°C. They found that the Fe^{3+}AlOH bending mode at 880 cm^{-1} disappeared with treatment by all of the reducing agents investigated. In each case the results indicated

reduction was accomplished by protonation of an adjacent OH group which was reversible upon oxidation with H_2O_2. The disappearance of the 885 cm^{-1} band occurred in our spectra when H_2 was added to the 8.6% Pt·Wy.montmorillonite at 140°C, but in this case it appears that the increase in layer charge is satisfied by the formation of the ammonium cation rather than protonation of hydroxyl groups. Calculation of the amount of ammonium formed when all of the octahedral iron (0.54 mmol Fe^{3+}/gm clay) is reduced plus the ammount of ammonium formed upon reduction of the platinum (0.882 mmol NH_4^+/gm clay) yields a value which agrees well with the amount predicted from the titration results (1.472 mmol/gm clay). The decrease in the hydroxyl stretching frequency observed with the concurrent high frequency shift or disappearance of the FeAlOH mode has been related to the reduction of structural Fe^{3+} (15). The presence of the metal ammine complex in the interlayer apparently facilitated the reduction of the octahedral iron, in part, by propping the interlayer apart, because an NH_4^+·Wy. montmorillonite, treated under the same reducing conditions as the 8.6% Pt catalyst, showed no change in its IR spectrum.

The changes in the IR spectra of the 0.6%, 1.0%, and 3.0% Pt·Wy.montmorillonite upon reduction are quite similar to the 8.6% Pt sample although the FeAlOH deformation band never completely disappeared. Rather, the decrease in intensity of the band was proportional to the metal content of the catalyst. As the results given above establish the involvement of the interlayer metal in the reduction of structural iron, this observation is not unexpected.

Several studies have established that Cu (II) square planar complexes adsorbed on Wy. montmorillonite orient with the metal-ligand bonds parallel to the silicate sheets and the vacant d_{z^2} metal orbital perpendicular to the interlamellar surface (16, 17). The 2.5Å interlayer separation observed for the 8.6% $Pt(NH_3)_4^{2+}$·Wy.montmorillonite would seemingly substantiate this orientation. By analogy, lower contents of $Pt(NH_3)_4^{2+}$ would also be expected to attain this configuration although X-ray data for these samples cannot confirm their orientations due to the uncertainty in the basal spacings.

It is evident that reduction of all catalysts produced a decrease in the interlayer spacing which under vacuum approached a value nearly identical to an evacuated NH_4^+·Wy. montmorillonite. In light of the TEM results, the reduction of the metal is envisaged as diffusion of metal atoms and crystallites out of the interlayer through the edge openings followed by distribution of individual crystallites to areas on the external clay surface and edge sites of lower electron density. Therefore, the narrowing of the (001) reflection with reduction of 0.6%, 1.0%, and 3.0% Pt catalysts resulted from an increase in the overall ordering or regularity of the interlayer dimension produced by the collective migration of the metal out of this region. This fact coupled with the collapse of all catalyst basal spacings to identical values rules out the probability that a high proportion of the metal remained in the mineral interlayer as individual atoms or crystallites. Indeed, a priori, the high charge density

found within the interlamellar regions would be expected to destabilize the metal and favor its redistribution to external surfaces.

TEM results clearly show that a small proportion of the reduced metal accumulates at the edges of the mineral after diffusion out of the interlayer. This apparently imparts limited swelling properties to the mineral upon rehydration at 97% RH. Table I-2 demonstrates that although the reduced Pt·Wy. montmorillonites are ammonium saturated, equilibration with water vapor did not restore the basal spacing to the value observed for a similarly treated NH_4^+·Wy. montmorillonite.

Conclusions

The results of this study have shown that interlayer $Pt(NH_3)_4^{2+}$ was readily reduced with hydrogen at 140°C according to the mechanism $Pt(NH_3)_4^{2+} + H_2 \rightarrow Pt° + 2NH_4^+ + 2NH_3$. The reaction was accompanied by the concurrent reduction of structural iron thereby increasing the layer charge of the mineral. Charge balance was maintained by the additional formation of ammonium cations produced by protonation of the ammine ligands.

After metal reduction, platinum atoms or crystallites migrated out of the interlamellar region and were distributed on the external surface and edge sites presumably of lower negative charge. At low metal loadings of 0.6% and 1.0% Pt, high dispersions were obtained with minimal pretreatment.

Reduction at higher metal loadings, however, resulted in poor metal dispersion and in many instances clustering of smaller crystallites into films of undetermined thickness. Nonetheless, approximately 50% of the crystallites examined were less than 30Å.

Finally, X-ray analysis demonstrated that the interlayer swelling capacity of the montmorillonite mineral is not completely impaired permitting suspension of the catalyst in solution and suggesting that this support might be particularly well-suited for condensed phase hydrogenations.

TABLE I-1
IR Band Frequencies for Pt Supported on Wy. Montmorillonite (cm^{-1})

Catalyst	Treatment[a]	ν(OH)	ν(NH)	δ(NH)	$\delta(Al_2OH)$	δ(FeAlOH)
0.6% Pt·Wy.montmorillonite	Untreated(RTP)	3625	3260	1425,1370	920	885
	Evacuated			1425,1345		
	Reduced	3625	3260	1425	920	885
1.0% Pt·Wy.montmorillonite	Untreated(RTP)	3625	3260,3220	1425,1370	920	885
	Evacuated			1425,1345		
	Reduced	3625	3260	1425	920	885
3.0% Pt·Wy.montmorillonite	Untreated(RTP)	3625	3300,3260,3220	1425,1370	920	885
	Evacuated			1425,1340		
	Reduced	3620	3260	1425	915	890
	RTP	3625			920	885
8.6% Pt·Wy.montmorillonite	Untreated(RTP)	3625	3290,3220	1370	920	885
	Evacuated		3330,3300,3220	1335		
	Reduced	3600	3260	1425	915	absent
	RTP	3625			920	885
NH_4^+·Wy.montmorillonite	Evacuated	3625	3260	1425	920	885

[a]Untreated refers to the cationic $Pt(NH_3)_4^{2+}$ form.
RTP represents room temperature and pressure conditions.

TABLE I-2
X-ray Analysis of Pt Loaded Wy. Montmorillonites

Catalyst	Treatment[a]	Basal Spacings (Å)			
		1st order	2nd order	3rd order	4th order
0.6% Pt·Wy.mont-morillonite	Untreated(RTP)	12.62	6.12	4.20	3.20
	Evacuated	10.68	5.31	--	2.62
	Reduced(97%RH)	13.85	6.87	--	3.52
	Evacuated	10.62	5.33	3.17	--
1.0% Pt·Wy.mont-morillonite	Untreated(RTP)	12.62	6.10	4.15	3.11
	Evacuated	10.77	5.32	--	2.67
	Reduced(97%RH)	13.25	6.66	--	3.35
	Evacuated	10.60	5.27	3.19	--
3.0% Pt·Wy.mont-morillonite	Untreated(RTP)	12.71	6.43	4.31	3.32
	Evacuated	11.51	--	--	2.85
	Reduced(97%RH)	12.66	6.33	--	3.16
	Evacuated	10.58	5.32	3.20	--
8.6% Pt·Wy.mont-morillonite	Untreated(RTP)	12.62	6.30	4.23	3.14
	Evacuated	12.05	6.00	--	3.04
	Reduced(RTP)	11.10	5.52	3.67	--
	Evacuated	10.64	5.21	3.14	--
	(97%RH)	12.27	6.10	--	3.08

[a]Untreated refers to the cationic $Pt(NH_3)_4^{2+}$ form.
RTP represents room temperature and pressure conditions.

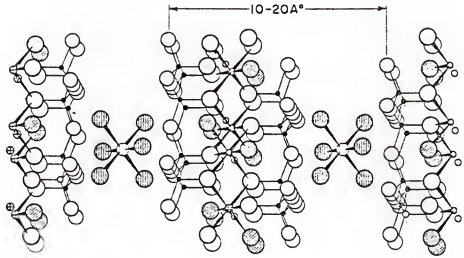

FIG. I-1. The structure of a smectite mineral illustrating the two tetrahedral silica sheets linked to the central octahedral sheet through oxygen apices. Shaded circles in the octahedral sheet represent hydroxyl groups bridge-bonded to adjacent structural cations. Hydrated cations are seen positioned between stacked smectite layers.

FIG. I-2a. Transmission electron micrograph of 0.6% Pt·Wy. montmorillonite shown at a magnification of 156,000x.

FIG. I-2b. Transmission electron micrograph of 1.0% Pt·Wy. montmorillonite shown at a magnification of 156,000x.

FIG. I-2c. Transmission electron micrograph of 8.7% Pt·Wy. montmorillonite shown at a magnification of 156,000x.

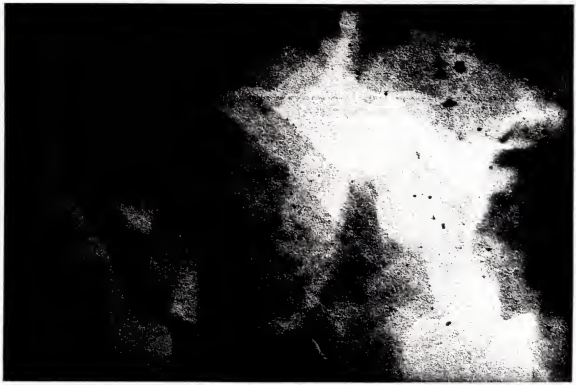

FIG. I-2d. Transmission electron micrograph of 3.0% Pt·Wy. montmorillonite shown at a magnification of 156,000x.

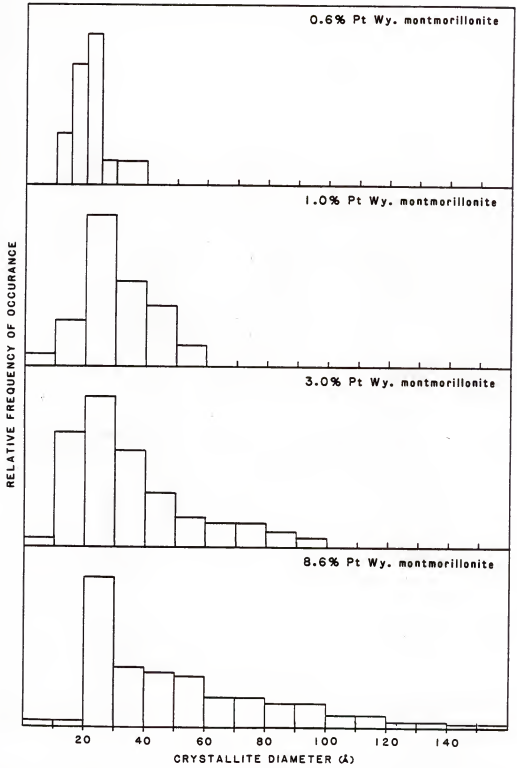

FIG. I-3. Particle size distributions for four loadings of platinum supported on Wy. montmorillonite. Metal crystallites larger than 160Å were counted in the last column.

CHAPTER II
HYDROGEN REDUCTION OF $Pd(NH_3)_4^{2+}$ SUPPORTED ON MONTMORILLONITE

Introduction

As early as the 1930s, acid-treated montmorillonites were used as catalyst supports for iron and nickel in the hydrocracking of middle oils (18). With the development of synthetic zeolites, their use declined until the late 1960s when synthetic mica-montmorillonite (SMM) was developed and patented by Granquist (19). The use of SMM as a support for hydrogenation metals did not occur until the 1970s when a number of patents were filed disclosing the development of a more effective light oil hydrocracking catalyst (19-25). However, despite the extensive issuance of patents, the use of layer silicate minerals as support materials for heterogeneous catalysis has been largely overlooked. In one exception, Pinnavaia and Welty (7) demonstrated that Rhodium (II) complexes supported on hectorite showed a higher catalytic activity toward 1-hexene hydrogenation than the same complex supported on a Dowex 50 resin or Rh_2^{4+} homogeneous solution.

The present study was initiated to characterize physical and chemical environment of $Pd(NH_3)_4^{2+}$ adsorbed on Wyoming

montmorillonite in four different concentrations and to elucidate the distribution and crystallite dimensions of the metal after reduction with dry hydrogen. The influence of the montmorillonite support on the electronic properties of the metal and its implications for catalytic activity were also investigated.

Experimental

Wyoming (Wy.) montmorillonite (CMS-SWY-1), purchased from the Source Clay Minerals Repository, University of Missouri, was washed with 1.0N NaOAc (pH 5.0) at 80°C to remove carbonates and then washed five times with NH_4Cl. Excess salts were removed by centrifugation and decantation with deionized water until chloride was undetectable with $AgNO_3$ in the supernatant. The <2 μm fraction was obtained by centrifugation and the resultant suspension dried at 110°C. The mineral has the structural formula

$$NH_4^+{}_{0.90}(Al_{3.07}Fe^{3+}_{0.41}Mg^{2+}_{0.31})(Si_{7.69}Al_{0.31})O_{20}(OH)_4 \cdot \quad \text{(Ref. 8)}$$

Palladium (II) was added as the tetrammine nitrate salt in four different concentrations corresponding to 0.6%, 1.0%, 3.0%, and 4.85% (w/w) with the latter representing the fully exchanged sample. Subsequent atomic absorption analyses of exchanged Na^+ confirmed the loading percentages.

Gas reagents used in this study were obtained from Linde Corporation in the highest grades possible. Hydrogen and

deuterium were further purified by passage through zeolite and liquid N_2 traps before being admitted to the sample container. Before reduction of the interlayer metal, the $Pd(NH_3)_4^{2+}$ montmorillonite was slowly heated to 140°C under vacuum (1×10^{-5} Torr). Vacuum was maintained for a minimum of 6 hours before addition of 100 Torr H_2 (or D_2). The sample was exposed to the static atmosphere of H_2 for 6 hours, evacuated to 1×10^{-5} Torr and reexposed to 100 Torr H_2 (or D_2) for another 6 hours. At this point, the sample was evacuated to less than 10^{-5} Torr and was ready for further treatment.

For infrared analysis, self-supporting films were made by drying a dilute suspension of the $Pd(NH_3)_4^{2+}$ loaded clay on mylar film. A stainless steel evacuable cell fitted with KRS-5 windows was used when recording IR spectra of samples in the presence of different gases. All spectra were recorded on a Perkin-Elmer 567 IR spectrophotometer.

X-ray analyses were performed with a Diano XRD-700 X-ray diffractometer using Ni-filtered Cu Kα radiation. Basal spacings were determined from at least three orders of reflection. Diffractograms of dehydrated clay films were obtained by transferral of the sample, under flowing dry He, from a vacuum cell to a glove bag attached to the X-ray sample mount.

Transmission electron micrographs were taken at magnifications ranging from 50K to 100K with a JEOL 100C electron microscope operated at 40KV. Average particle diameters for

each loading were computed by using a statistically weighted area average:

$$\bar{d}_s = \frac{\Sigma n_i d_i^3}{\Sigma n_i d_i^2} \qquad \text{(Ref. 8)}$$

Results

Infrared Spectroscopy

Although four different loadings of palladium were used in this study, with only a few exceptions noted below, the IR spectra of the fully loaded 4.7% Pd·Wy. montmorillonite reflected the status of the metal complex for the lower Pd concentrations as well. It is for this reason that the major portion of results reported here will be devoted to the fully loaded mineral.

The infrared bands which appeared in the IR spectrum when $Pd(NH_3)_4^{2+}$ was completely exchanged for NH_4^+ are shown in Fig. II-1 and listed in Table II-1. The triplet at 3320, 3280, and 3200 cm^{-1} in the spectrum of the air-dry film, ascribed to NH stretching vibration of the ammine ligand (12, 13), shifted slightly to 3340, 3270, and 3195 cm^{-1} upon evacuation. The corresponding symmetric bending fundamental shifted from 1305 cm^{-1} to 1270 cm^{-1} with decreasing hydration levels. The degenerate antisymmetric deformation, while obscured by the overlapping H_2O bending fundamental in the spectrum of the air-dried mineral, was observed at 1630 cm^{-1} when the sample was thoroughly dehydrated under vacuum.

All vibrations associated with the Wy. montmorillonite mineral have been previously assigned (10) and are listed with the cation fundamentals in Table II-1. The (Pd-N) stretching and (N-Pd-N) bending fundamentals were not observed in our spectra due to strong overlapping bands associated with the montmorillonite skeletal modes in the region between 550 cm^{-1} and 250 cm^{-1}.

The IR spectra of lower Pd loadings closely resembled the fully loaded sample albeit in the 0.6% and 1.0% Pd·Wy. montmorillonite a strong NH vibration at 3260 cm^{-1}, associated with the residual NH_4^+ cation, obscured bands resulting from ammine stretching vibrations.

In all samples the addition of 100 Torr H_2 in 2 exposures over a 12-hour period resulted in the appearance of 2 broad bands at 3260 cm^{-1} and 1425 cm^{-1}, and a concurrent disappearance of all bands associated with the ammine ligands (Fig. II-1). Several obvious changes were observed in vibrations originating with the montmorillonite mineral. In particular, a 20 cm^{-1} downward shift in ν(OH) and a complete disappearance of the FeAlOH bending mode were observed for the 4.7% Pd·Wy.montmorillonite upon reduction of the interlayer metal. Exposure of the sample to room atmosphere restored all mineral vibrations to their original positions and intensities.

Exposure to H_2 at 140°C produced similar changes in the mineral lattice vibrations of the 0.6%, 1.0%, and 3.0% Pd·montmorillonites. However, in contrast to the fully exchanged clay, there was no shift in the ν(OH) for the lower loadings,

and the Fe Al OH bending mode appeared to only decline in intensity in proportion to the metal content. Again, with exposure to room atmosphere the bending fundamental was restored to its initial intensity and position.

To further elucidate the reduction mechanism and the concurrent manifestations in the IR spectra, D_2 was substituted for hydrogen as the reducing agent. As seen in Fig. II-2, interlayer metal reduction is accompanied by deuteration of a portion of the structural hydroxyls and the formation of $(NH_xD_{4-x})^+$ species for which there are two broad vibrations at 3280 cm^{-1} and 2440 cm^{-1}. The latter bands exhibited the expected isotope shift of 1.34 ($^{\nu N-H}/_{\nu N-D}$). Absorbance peak area measurements revealed a reduction in the ν(OH) of approximately 23% when D_2 was substituted for H_2. This is exactly equal to the ratio of layer charge to the number of hydroxyls in the unit cell formula for the montmorillonite. Curiously, hydroxyl deuteration, observed in the stretching region of the IR spectrum, was not manifested in the bending region as a disappearance or shift of any particular hydroxyl combination. Rather, when the spectrum was recorded in the absorbance mode, apparent decreases in band intensities were observed for the bending modes of all cation-hydroxyl combinations.

X-ray Analysis

Basal reflections for all loadings of palladium are listed in Table II-2 with their respective treatments. Although, under evacuated conditions, each loading of $Pd(NH_3)_4^{2+}$ showed

a similar interlamellar spacing the first and higher order reflections increased in breadth with decreasing metal content demonstrating the random interstratification expected for non-homoionic preparations.

A pronounced decrease in the basal spacing and peak width occurred with all samples treated with H_2 at 140°C. In fact, under vacuum conditions all palladium loaded samples showed basal spacings equivalent to an NH_4^+ saturated Wy. montmorillonite. X-ray scans over the angles expected for the 111, 200, 220, and 311 reflections of crystalline palladium revealed a diffuse and poorly defined peak at 40.14° 2θ for the fully saturated Pd·Wy.montmorillonite. Unquestionably, this was the 111 reflection indicative of Pd cluster formation. High noise levels at sensitive instrument settings combined with the uncertainty in peak width made line broadening measurements of crystallite size impractical. There was no indication of cluster formation in any of the other samples after reduction.

Transmission Electron Microscopy (TEM)

Transmission electron micrographs of reduced Pd·Wy.montmorillonites prepared as described above are shown in Fig. II-3. Corresponding particle size distributions, deduced from electron micrographs, are shown in Fig. II-4. It is evident from these figures that a narrow size distribution was obtained for the 0.6% Pd·montmorillonite, with all particles forming in crystallites of 50Å or less. Over 95%

of these particles were less than 30Å and had a mean diameter of 30.9Å. Increasing the palladium concentration to 1.0% produced a pronounced broadening of the distribution with the occasional appearance of crystallites in the 70-90Å range. At this loading only 58% of the particles examined were less than 30Å and 88% less than 50Å. By including all particles in the mean diameter calculation, a value of 44.9Å was obtained. However, when counting only those less than 50Å (88% of the sample population) the mean diameter was 37.2Å. At the 3.0% Pd level only 50% of the sample population was less than 30Å; yet nearly 80% were less than 50Å. Despite a high proportion of particles less than 50Å, the mean particle diameter was 86.2Å reflecting the influence of the larger particles on the mean diameter calculation. When the mineral was fully exchanged with palladium and reduced, large metal clusters appeared with diameters occasionally exceeding 200Å. Nonetheless, 44% of the crystallites examined were less than 30Å and 67% less than 50Å. All particles included, the mean diameter at this loading was 121.6Å.

These results demonstrate the expected decrease in palladium dispersion as the metal content was increased. Indeed, a small incremental increase in palladium content (from 0.6% to 1.0% Pd) was accompanied by a pronounced broadening in the particle diameter distribution curves (Fig. II-4). This appears to be an artifact of the diffusion of metal atoms or crystallites formed upon metal cation reduction, from the interlayer to edge and external surface sites.

Discussion

In most cases, knowledge of the symmetry of a molecule and selection rules allows the prediction of the number of infrared active fundamentals which should appear in the IR spectrum. A noncorrespondence between the number of predicted bands and the number of observed vibrations can only indicate a change in the geometrical configuration or symmetry of the molecule. A number of studies have shown that the $Pd(NH_3)_4^{2+}$ complex possesses D_{4h} symmetry (26, 27). However, since only the ligand vibrations are observable when the molecule is exchanged on Wy. montmorillonite, it is more useful to evaluate the symmetry of ligands independently. This is accomplished by viewing the NH_3 group vibrations as a simple 1:1 (metal/ligand) model with C_{3v} local symmetry (12). In this point group, two stretching fundamentals (the doubly degenerate antisymmetric and the symmetric vibrations) and two bending fundamentals (antisymmetric and symmetric) are predicted to be infrared active. An examination of Fig. II-1 and Table II-1 clearly shows three stretching fundamentals were observed in the IR spectrum of the air-dried fully exchanged $Pd(NH_3)_4^{2+}$ montmorillonite. The observed triplet reflects a 40 cm^{-1} splitting of the doubly degenerate stretching fundamental which must have accompanied a reduction in symmetry of ligands with loading on the mineral. Thorough evacuation of the sample increased the splitting of antisymmetric fundamental to 70 cm^{-1} indicating further symmetry

reduction. These results can be explained in terms of a strong interaction of the ammine ligand with the interlayer silicate sheet which increased with evacuation. The 2.5Å interlamellar spacing observed from X-ray analysis suggests the complex retained its square planar configuration when evacuated, thereby increasing the possibility that the NH_3 ligands were experiencing limited rotation about the C_{3v} axis when adsorbed in the mineral interlayer. Restricted rotation, increasing with evacuation, produces a reduction in symmetry of the ligands. This is manifested in the IR spectrum as a splitting of the antisymmetric stretching fundamental, which increases with further symmetry reduction. Due to the low intensity of the corresponding antisymmetric bending fundamental at 1630 cm^{-1}, it is uncertain whether there was a splitting of this vibration too. The symmetric bending mode, particularly sensitive to the hydration level of the mineral, shifted from 1305 cm^{-1} to 1270 cm^{-1} with evacuation. A shift of this magnitude is expected for decreasing hydrogen bonding between interlayer water and the ammine ligands (13).

It was pointed out in the results section that reduction of the interlayer metal complex to zero valency resulted in a complete disappearance of all the ammine vibrations and the appearance of single bands at 3260 cm^{-1} and 1425 cm^{-1}. Comparisons of this spectrum with an NH_4^+ saturated montmorillonite confirmed the formation of ammonium as part of the reduction mechanism. This conclusion was reinforced by the decrease in the basal spacings of all reduced and evacuated

samples to a value equivalent to an evacuated NH_4^+ saturated mineral.

Several important points were revealed in the IR spectrum by substituting D_2 in the reduction process. First, the formation of OD in a ratio equivalent to the layer charge/number of hydroxyls in the half-cell formula established that D_2 diffused into the interlayer rather than reduction of the metal occurring at the edges of the mineral and progressing inward. Second, two separate studies have demonstrated that in square planer Cu(II) complexes on Wy. montmorillonite, the vacant d_{z2} orbital is oriented toward and coordinated to surface silicate oxygens (16, 17). Therefore, we propose that during reduction, electron transfer from D_2 to $Pd(NH_3)_4^{2+}$ proceeded via the vacant d_{z2} orbital forming a pair of deuterons (D^+), one of which readily exchanged with a structural hydroxyl in close proximity to the Pd center. The second deuteron and the exchanged proton (from the structural hydroxyl) were immediately scavanged by two ammine ligands. This is consistent with the formation and appearance in the IR of $(NH_xD_{4-x})^+$ species.

In addition to ammonium formation, the addition of H_2 (or D_2) at 140°C resulted in the reduction of structural Fe (III) as demonstrated by the disappearance of the δ(AlFeOH) band. This is not surprising since Rozenson and Heller-Kallai (8, 14) reported a similar result when octahedral iron reduction was accomplished by using aqueous solutions of hydrazine, sodium dithionite, and sodium sulfide at 70°C.

However, an NH_4^+-montmorillonite exposed to H_2 at 140°C for 12 hours showed no variation in its IR spectrum. Thus, the presence of the interlayer metal complex facilitated the reduction of structural iron. In addition, it appears that the resultant increase in layer charge is satisfied by the additional conversion of ammine to ammonium. In an earlier work we demonstrated that the amount of ammine retained by the mineral as ammonium was equivalent to that predicted by the stoichiometry of reduction plus the increase in layer charge (Chap. I).

The IR spectroscopic results have established that the metal is reduced within the interlamellar region, while TEM results have clearly shown the distribution of the metal as crystallites on the external surface and edges. Therefore, it is reasonable to assume that due to high interlamellar charge, palladium atoms or crystallites diffused out of the interlayer upon reduction and redistributed on the external surface and edge sites at points of lowest surface charge. Furthermore, the strong dependence of crystallite size on metal loading concentrations infers that crystallite formation occurred as the metal diffused out of the interlayer and/or at the edge sites rather than on the external surface. One exception to this concept occurred at the highest metal loading where an electron micrograph showed the subsequent fusion of large clusters which appeared as dark bands or films. Coalescence of metal particles occurs when the affinity for a neighboring particle exceeds the stability exerted by the

support. However, support effects would be expected to decline as particle size increases.

Particle size distributions (Fig. II-4) deduced from electron micrographs display the relatively narrow particle size range obtainable at low metal concentrations. It is important to note that film grain sizes limited observable particles to larger than 10Å, thereby increasing the likelihood that the average particle diameters were overestimated. Although the average particle size and the size distribution increase with metal concentrations, it is evident that a large percentage of the particles formed in diameters of 30Å or less. This is obviously an important point from the perspective of attaining high metal surface areas.

Conclusions

Tetrammine palladium (II) exchanged on an NH_4^+·montmorillonite at various weight percentages has shown a strong interaction between the silicate interlayer and ligand groups in air-dried and evacuated states as deduced from symmetry concepts applied to infrared spectra. X-ray results suggest that the complex retains its D_{4h} symmetry with the ammine ligands parallel to the interlayer and the empty d_{z2} metal orbital oriented perpendicular to the sheets.

Reduction of the interlayer complex results in the formation of Pd(O) atoms and/or crystallites which migrate out of the interlamellar region and redistribute on the external

surface and at edge sites of low negative charge. Low metal loadings of 0.6% and 1.0% Pd produced high metal dispersions with narrow size distributions. Higher concentrations of metal resulted in relatively broad particle size distributions and large crystallite diameters. In some cases, crystallites deposited in close proximity to one another subsequently clustered and formed films of undetermined thickness. Under these circumstances the metal showed a greater affinity for a neighboring particle than for the mineral surface.

Finally, the high metal surface areas obtained at low palladium loadings coupled with the swelling properties of the mineral suggest these materials may be well suited for condensed phase hydrogenations where catalyst suspension would reduce inherent diffusion gradients.

TABLE II-1
IR Band Frequencies for Pd Supported on Wy. Montmorillonite (cm^{-1})

Catalyst	Treatment[a]	ν(OH)	ν(NH)	δ(NH)	δ(Al_2OH)	δ(FeAlOH)
0.6% Pd·Wy.mont-morillonite	Untreated(RTP) Evacuated	3625	3260	1425,1305 1425,1270	920	885
	Reduced	3625	3260	1425	920	885
1.0% Pd·Wy.mont-morillonite	Untreated(RTP) Evacuated	3625	3260	1425,1305 1425,1270	920	885
	Reduced		3260	1425	920	885
3.0% Pd·Wy.mont-morillonite	Untreated(RTP) Evacuated	3625	3280 3340,3260,3200	1425,1305 1425,1270	920	885
	Reduced	3620	3260	1425	915	890
4.7% Pd·Wy.mont-morillonite	Untreated(RTP) Evacuated	3625	3320,3280,3200 3340,3270,3200	1305 1270	920	885
	Reduced RTP	3605 3625	3260	1425	912	absent

[a]Untreated refers to the cationic $Pd(NH_3)_4^{2+}$ form.
RTP represents room temperature and pressure conditions.

TABLE II-2
X-ray Analysis of Pd Loaded Wy. Montmorillonites

Catalyst	Treatment[a]	Basal Spacings (Å)			
		1st order	2nd order	3rd order	4th order
0.6% Pd·Wy.montmorillonite	Untreated(RTP)	12.75	6.43	--	--
	Evacuated	10.95	5.50	--	--
	Reduced(97%RH)	12.65	6.32	4.18	3.21
1.0% Pd·Wy.montmorillonite	Untreated(RTP)	12.80	6.40	--	--
	Evacuated	11.33	5.67	--	--
	Reduced(97%RH)	12.60	6.41	4.20	--
3.0% Pd·Wy.montmorillonite	Untreated(RTP)	12.77	6.38	--	3.18
	Evacuated	11.80	6.05	3.92	2.95
	Reduced(97%RH)	12.55	6.20	4.20	3.11
4.7% Pd·Wy.montmorillonite	Untreated(RTP)	12.80	6.34	4.25	3.15
	Evacuated	12.12	6.03	4.10	3.03
	Reduced(97%RH)	12.25	6.16	4.10	3.05
	Evacuated	10.40	5.25	3.50	--

[a]Untreated refers to the cationic $Pd(NH_3)_4^{2+}$ form.
RTP represents room temperature and pressure conditions.

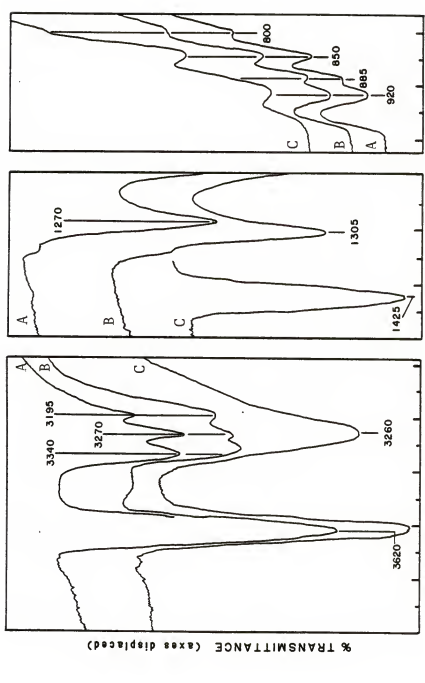

FIG. II-1. Infrared spectra of fully loaded (4.7% Pd) Wy, montmorillonites: (A) evacuated $Pd(NH_3)_4^{2+}$ sample, (B) air-dry $Pd(NH_3)_4^{2+}$ sample, (C) after hydrogen reduction at 140°C.

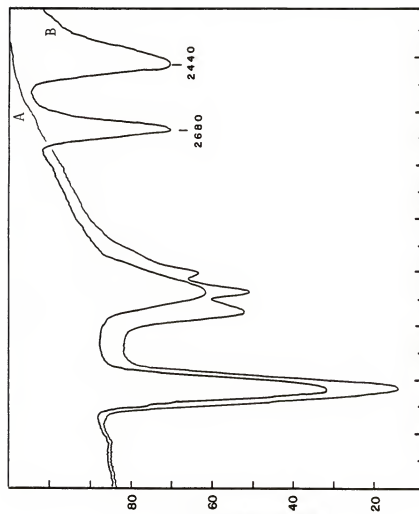

FIG. II-2. Infrared spectra of fully loaded (4.7% Pd) Wy. montmorillonites: (A) evacuated $Pd(NH_3)_4^{2+}$ sample, (B) after reduction with D_2 at 140°C.

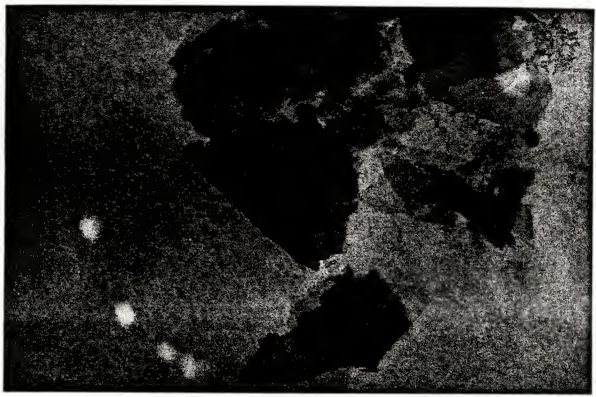

FIG. II-3a. Transmission electron micrograph of 0.6% Pd·Wy. montmorillonite shown at a magnification of 156,000x.

FIG. II-3b. Transmission electron micrograph of 1.0% Pd·Wy. montmorillonite shown at a magnification of 156,000x.

FIG. II-3c. Transmission electron micrograph of 3.0% Pd·Wy. montmorillonite shown at a magnification of 156,000x.

FIG. II-3d. Transmission electron micrograph of 4.7% Pd·Wy. montmorillonite shown at a magnification of 156,000x.

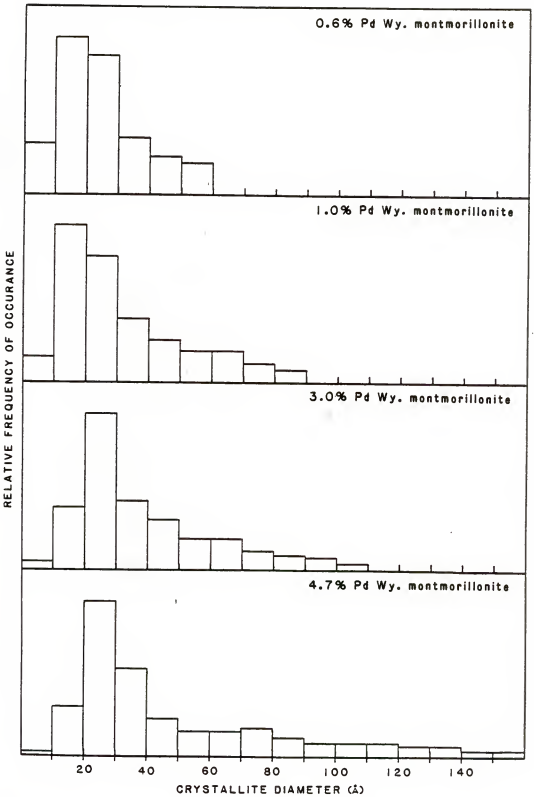

FIG. II-4. Particle size distributions for four loadings of palladium supported on Wy. montmorillonite. Metal crystallites larger than 160Å were counted in the last column.

CHAPTER III
MOLECULAR HYDROGEN INTERACTION WITH LAYER SILICATE SUPPORTED Pd AND Pt CATALYSTS

Introduction

In the past, selective gas chemisorption has been utilized for the physical characterization of supported metal catalysts. Typically, the estimation of exposed metal surface areas and the extents of dispersion have been determined by volumetric measurements of H_2, O_2, and CO gas uptake and an assumption of the stoichiometry for the reaction between the gas and surface metal atom. Benson and Boudart (28) proposed the O_2-H_2 titration technique as an alternative chemisorption method which had the advantages of minimal catalyst pretreatment and the possibility of a threefold increase in sensitivity over standard chemisorption measurements. Based on chemisorption data collected for H_2, O_2, and the H_2-O_2 titration, the authors proposed a stoichiometry of $M_s\text{-}O + \frac{3}{2} H_2 \rightarrow M_s\text{-}H + H_2O_{(ads)}$ where an oxygenated metal surface exposed to dry hydrogen at room temperature resulted in a metal surface covered with atomic hydrogen in a 1:1 ratio and the formation of water subsequently adsorbed by the support. Despite a number of studies which have found a good correspondence between metal dispersions determined

by the titration method and other physical methods, there is a general disagreement in the literature as to the exact stoichiometry of the titration reaction and factors which might influence the outcome (29, 30). Kikuchi et al. (31) found an apparent enhancement of hydrogen adsorption with repeated O_2-H_2 titrations and postulated that the generated H_2O was the possible cause for the effect. Promotion of hydrogen uptake can result in an overestimation of metal dispersion and has been collectively referred to as "hydrogen spillover" (32). Although no specific examples of hydrogen spillover have been reported for metal dispersions determined by the titration technique, the phenomenon is not uncommon when using standard gas chemisorption methods (reviewed in Ref. 32).

In light of the minimal attention directed toward the occurrence of hydrogen spillover during O_2-H_2 titrations, this study was initiated to elucidate some of the factors which contribute to the enhancement of dissociative hydrogen chemisorption during the titration of palladium and platinum supported on a naturally occurring clay mineral. For the specific purpose of comparison, this study also presents infrared and gravimetric data for the independent adsorption of carbon monoxide.

Experimental

The preparation and subsequent reduction procedures for 0.6%, 1.0%, 3.0%, and fully exchanged (0.85 meq/gm clay) palladium and platinum Wyoming (Wy.) montmorillonites were described in Chapters I and II.

All gas reagents were obtained from Linde Corporation in the highest grades available and used without further purification with the exceptions of hydrogen and deuterium which were passed through a zeolite-liquid N_2 trap prior to use. Alumina supported Pd and Pt were purchased from Alpha-Ventron Corporation and used as received.

Metal dispersion (number of exposed surface atoms/total number of metal atoms) was determined gravimetrically by use of the O_2-H_2 titration techniques of Benson and Boudart (28), water loss measurements after the titration, and CO chemisorption.

The general procedure followed for dispersion measurements of prereduced samples (~100 mg) consisted of a 12 hour evacuation period at 5×10^{-6} Torr and 25°C, followed by exposure of the sample to 75 Torr O_2 for 12 hours, and evacuation another 12 hours at 5×10^{-6} Torr. Sixty Torr of D_2 (or H_2) was introduced into the system and maintained for 6-12 hours. Each sample was then outgassed for 6 hours at 5×10^{-6} Torr to measure the amount of water lost. Finally, the sample, assumed to be deuterium (or hydrogen saturated),

was exposed to 60 Torr CO for 6 hours. This procedure was repeated a minimum of three times on the same sample with readings taken after each treatment.

The silica spring adsorption balances used in all gravimetric determinations have been discussed in theory and practice by Berkheiser et al. (33). A diagram of the adsorption apparatus is shown in Fig. III-1 (adapted from Ref. 36). A constant temperature of 25° ± 0.01°C was maintained by a Lauda model K-4R circulator pump flowing a water-ethylene glycol solution through the thermostatic cooling/heating jacket surrounding each adsorption tube. Spring lengths ($\Delta\ell$) were measured by a model 2207 cathetometer manufactured by the Precision Tool and Instrument Company, Ltd. Gas pressure at high vacuum was measured by a CVC model GPH 324C Penning ionization gauge, and in the range of 0.01 Torr to 100.00 Torr by a MKS Instruments Inc. model 220 capacitance manometer. A vacuum of 1×10^{-6} Torr was achieved in our glass apparatus by a rotary roughing pump, an Edwards model 63/150 Diffstak oil diffusion pump, and a liquid N_2 trap positioned between the adsorption tubes and the vacuum pumps.

Results

Both CO chemisorption and the O_2-H_2 titration technique were utilized in this study to offer two independent evaluations of metal dispersion and to elucidate the behavior of the montmorillonite support during gas adsorption measurements.

The gravimetric determination of metal dispersions by the hydrogen titration of chemisorbed oxygen has several advantages over volumetric methods in that it provides two independent means for calculating the ratio of the number of exposed metal atoms to the total number of metal atoms present during catalyst loading. Because the stoichiometry of the titration reaction requires one H_2O molecule per surface metal atom, it should be possible to estimate the metal dispersion by the in vacuo weight loss of H_2O provided the water is not chemisorbed by the support. Therefore, metal dispersions in the present study were calculated by separate measurements of the weight change with addition of hydrogen and by the weight loss of water with thorough evacuation. For at least two replications of each titration, deuterium was substituted for hydrogen as the titrant thereby increasing the sensitivity of gravimetric measurements twofold. Average dispersion values with their respective standard deviations are shown in Table III-1 for the four loadings of Pd and Pt on Wy. montmorillonite. While a good agreement was obtained between dispersions determined by H_2O loss and TEM measurements (Chap. I,II) there was an unquestionable tendency by the titration procedure to overestimate the amount of exposed metal.

Although CO chemisorption was used in this study for dispersion determinations, the bonding habit of the molecule with the metal surface could not be predicted ab initio. In general, ν(CO) bands appearing in the 2130 to 2000 cm^{-1} region have been ascribed to linearly bonded species while those

appearing in the 2000 to 1850 cm^{-1} region have been assigned to bridging configurations (34). It is evident from the infrared spectra shown in Figs. III-2a and 2b, III-3a and 3b, and the data compiled in Table III-2, that at pressures equivalent to those used for dispersion measurements, CO was bonded to montmorillonite supported Pt in a 1:1 ratio (Pt-CO) and to palladium in a 1:2 ratio (Pd_2CO). These ratios were employed in the stoichiometry used for calculating the dispersions shown in Table III-1.

Interestingly, at low metal loading, the data obtained from CO chemisorption approached the range of dispersions determined by H_2O loss and TEM, but this correspondence fell off rapidly as the metal concentration increased.

To isolate the factors which contributed to the excessively high dispersion values obtained by the hydrogen titration of oxygenated metal supported on Wy. montmorillonite, a compilation of gravimetric data is presented in Table III-3. Using dispersion data calculated from TEM measurements, an expected change in weight for a known weight of catalyst can be calculated for the titration reaction stoichiometry proposed by Benson and Boudart (28). These expected values appear in column B of Table III-3. Subtracting this value from the observed weight change per weight of catalyst gives the weight of excess H_2 adsorption per mg catalyst (hydrogen spillover) shown in the last column of Table III-3. It is evident that, when expressed in this manner, there is a relatively constant excess uptake of H_2 independent of metal

content or metal species. With regard to this point, an ammonium saturated Wy. montmorillonite blank showed no change in weight throughout all H_2 titration and CO chemisorption experiments. Therefore, we conclude that the weight changes observed for metal loaded montmorillonites were not a result of surface contamination or an activity by the support alone. Also notable from Table III-3 is the negligible amount of hydrogen spillover for the titration of our control samples (alumina supported metals). Indeed, these results, for the alumina supported metals, seemingly confirm the validity of our experimental measurements and procedures. By taking the atomic weight of molecular hydrogen as 2.00 mg/mmol and an average for both metals, the excess uptake can be expressed in terms of mol H_2 excess uptake/g catalyst. In this form the amount of molecular hydrogen chemisorbed by a spillover mechanism is 2.37×10^{-4} mol H_2/g catalyst.

Discussion

Dissociative molecular hydrogen adsorption can be accompanied by the migration of hydrogen atoms from the surface of the metal to another phase of the catalyst which has hydrogen acceptor sites (35). Benson et al. (36), studying the reduction of tungsten trioxide, found that the presence of Pt metal and H_2O promoted the reduction of the oxide at room temperature. They postulated that water acted as a carrier by spreading the reducing species over the internal

surface of the tungsten oxide particles. Popova and Sokolskii (37) showed that iron impurities in Al_2O_3 resulted in a dramatic increase in the ratio of hydrogen adsorption to metal content during dispersion measurements. From these selected studies it is apparent that the presence of a noble metal, a carrier substance, and electron acceptor sites collectively contribute to the spillover of atomic hydrogen to the support phase. It is with this perspective that we shall explain our titration results.

Wyoming montmorillonites are sheet-silicates composed of units of two silica tetrahedral sheets linked by oxygen apices to a central aluminum octahedral sheet (Fig. III-4). The isomorphic substitution of ions of lower valence in the octahedral sheet and occasionally in the tetrahedral sheet imparts a negative charge to the mineral structure which is balanced by hydrated cations which reside in the interlamellar region. The mineral is also characterized by small amounts of structural iron (III) randomly distributed throughout the octahedral sheet. The approximate structural formula for the Wyoming montmorillonite is

$$Mo^{+}_{0.90}(Si_{7.69}Al_{0.31})(Al_{3.07}Fe^{3+}_{0.41}Mg_{0.51})O_{20}(OH)_4 \quad \text{(Ref. 8)}$$

Calculated from this formula, the average iron content of the Wy. montmorillonite is 5.74×10^{-4} mol Fe (III)/gm clay. Assuming that the structural iron is reducible by isolated hydrogen atoms according to the stoichiometry Fe (III) + H → Fe (II) + H^+, the amount of molecular hydrogen required is

2.87×10^{-4} mol H_2/gm montmorillonite. This value is remarkably close to the average value of spiltover hydrogen we observed for our H_2 titrations. In fact, an infrared study conducted concurrently with the titration procedures reveals iron (III) reduction as the primary source of hydrogen spillover on our catalysts. Figure III-5 shows the IR bending modes arising from hydroxyls bridging adjacent cations in the octahedral sheet of the mineral. According to the assignments of Farmer (10), the bands at 920, 890, 850, and 800 cm^{-1} are ascribed to the bending vibrations of $\delta(Al_2OH)$, $\delta(AlFe^{3+}OH)$, $\delta(AlMg^{2+}OH)$, and $\delta(Mg^{2+}Fe^{3+}OH)$, respectively. The IR spectra demonstrate the changes in the δ(AlFeOH) fundamental vibration when 60 Torr D_2 is admitted to a sample pretreated with oxygen. Rozenson and Heller-Kallai (8, 13) have reported a similar effect when a Wy. montmorillonite was treated with aqueous solutions of hydrazine, sodium dithionite, and sodium sulfide at 70°C.

In the two previous Chapters we established that a high proportion of the metal crystallites reside on the external surfaces and edge sites of the montmorillonite support, and residual ammonium cations are situated at sites of negative charge on the interlayer surfaces. Therefore, we propose that during the titration reaction, hydrogen atoms generated by dissociative molecular hydrogen adsorption migrated into the interlamellar region via generated water molecules effecting a reduction of the structural iron associated with the montmorillonite. Although electron transfer through the

interlayer has been implicated in the reduction of structural iron (8), it is not clear from our results whether this occurs in our system. However, evidence for proton and/or hydrogen atom migration was found when an oxygenated metal surface supported on an NH_4^+ saturated montmorillonite was exposed to D_2 during titration experiments (Fig. III-6). This resulted in the formation and subsequent increase with time in the ν(N-D) vibration at 2400 cm^{-1}. The sharp absorption at 2680 cm^{-1} has been ascribed to the mineral ν(OD) vibration produced during metal reduction with D_2 (Chap. II). Since the ammonium cation (NH_4^+) resides primarily within the mineral interlayer, N-D formation could only occur by the migration of deuterium oxide and/or free deuterium atoms from metal sites on the external surface of the clay into the interlamellar region.

The IR evidence of structural iron reduction with the concurrent formation of interlayer N-D species strongly suggests that dissociative molecular hydrogen adsorption is accompanied by the migration of "solvated" hydrogen atoms into the interlamellar spaces of the Wy. montmorillonite. This mechanism is consistent with previous investigations of structural iron reduction in Wy. montmorillonite (8, 13, Chaps. I, II) and explains the extraordinarily high dispersion values observed in our study for the H_2 titration of oxygenated metals supported on Wy. montmorillonites.

Conclusions

The application of O_2-H_2 titrations to Wy. montmorillonite supported palladium and platinum results in an overestimation of metal dispersion, primarily due to the phenomenon of hydrogen spillover. IR and gravimetric results have established the role of structural iron, present in the support phase, as hydrogen atom acceptor sites. In addition, it appears that water, generated during the titration reaction, acts as a carrier (envisaged as a H···H-OH interaction) permitting hydrogen atom migration into the interlamellar region of the mineral effecting a reduction in structural iron.

Despite the occurrence of hydrogen spillover during the titration reactions, reasonable estimates of dispersion were obtained in our gravimetric system by measurements of water loss and/or CO adsorption. These measurements provided a convenient, yet independent method for the analysis of exposed metal surfaces.

TABLE III-1
DISPERSION MEASUREMENTS FOR Pd and Pt MONTMORILLONITES

Catalyst	Dispersion (M_s/M_{total})			
	Hydrogen Titration	H_2O Loss	CO Chemisorption	TEM[a]
0.6% Pd	2.56±.22	0.47	0.52	0.39
1.0% Pd	2.53±.16	0.25	0.49	0.22
3.0% Pd	0.56±.25	0.16	0.40	0.10
4.7% Pd	0.49±.14	0.11	0.30	0.05
5.0% Pd/Al_2O_3	0.44±.07	0.39	0.45	0.55
0.6% Pt	4.69±.36	0.55	0.39	0.44
1.0% Pt	3.04±.15	0.20	0.29	0.24
3.0% Pt	1.00±.05	0.13	0.22	0.08
8.6% Pt	0.30±.17	0.10	0.18	0.03
5.0% Pt/Al_2O_3	0.49±.09	0.53	0.39	0.48

[a]Mean particle diameters from Chaps. I and II were converted to dispersion values by the equation of Aben (44).

TABLE III-2
CO BAND POSITIONS (P=60 Torr) OF
Pd AND Pt MONTMORILLONITES

Sample	ν(CO) (cm^{-1})	$\bar{d}$(Å)[a]
0.6% Pd	1930,1825(sh)	30.9
1.0% Pd	1930,1910(sh),1880(sh)	44.9
3.0% Pd	1935(b),1910(sh), 1885(sh),1750(b)	86.2
4.7% Pd	1950,1900, 1850(b),1750(sh)	121.6
0.6% Pt	2042	22.9
1.0% Pt	2050	42.7
3.0% Pt	2060	97.9
8.6% Pt	2065	158.6

[a]Average particle diameter ($\bar{d}$) determined from TEM measurements (Chaps. I and II).

TABLE III-3
ANALYSIS OF GRAVIMETRIC H_2 TITRATION DATA

Catalyst	Dispersion (TEM)	A: Observed $\Delta\omega t.$ $\left(\frac{mg}{wt.\ Catalyst}\right)$ $\left(\frac{mg}{mg}\right)$	B: Expected $\Delta\omega t.$ x Dispersion[a] $\left(\frac{mg}{wt.\ Catalyst}\right)$ $\left(\frac{mg}{mg}\right)$	Excess H_2 Uptake $\left(\frac{mg}{wt.\ Catalyst}\right)$ $\left(\frac{mg}{mg}\right)$ = A-B
0.6% Pd·Wy.montmorillonite	0.39	3.88×10^{-4}	5.92×10^{-5}	3.28×10^{-4}
1.0% Pd·Wy.montmorillonite	0.22	5.21×10^{-4}	4.52×10^{-5}	4.76×10^{-4}
3.0% Pd·Wy.montmorillonite	0.10	8.12×10^{-4}	1.44×10^{-5}	6.68×10^{-4}
4.7% Pd·Wy.montmorillonite	0.05	6.49×10^{-4}	6.62×10^{-5}	5.83×10^{-4}
5.0% Pd·Al_2O_3	0.55	6.19×10^{-4}	7.74×10^{-4}	-1.55×10^{-4}
			AVERAGE:	5.14×10^{-4}
0.6% Pt·Wy.montmorillonite	0.44	4.33×10^{-4}	4.06×10^{-5}	3.92×10^{-4}
1.0% Pt·Wy.montmorillonite	0.24	4.28×10^{-4}	3.38×10^{-5}	3.94×10^{-4}
3.0% Pt·Wy.montmorillonite	0.08	4.36×10^{-4}	3.45×10^{-5}	4.01×10^{-4}
8.6% Pt·Wy.montmorillonite	0.03	6.11×10^{-4}	6.10×10^{-5}	5.50×10^{-4}
5.0% Pt·Al_2O_3	0.49	7.53×10^{-4}	7.38×10^{-4}	1.48×10^{-5}
			AVERAGE:	4.34×10^{-4}

[a] Expected $\Delta\omega t.$ equals the wt. change expected for a dispersion of 1.0.

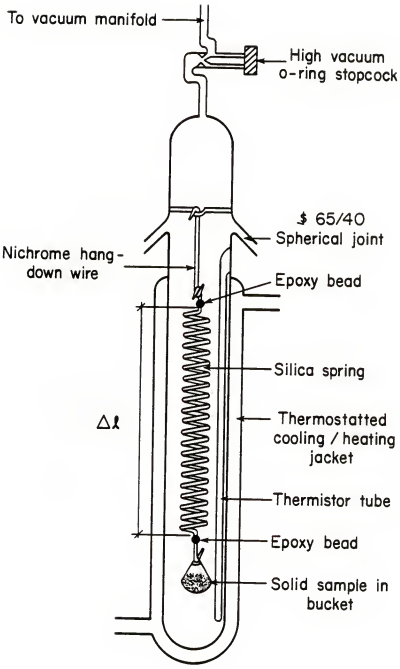

FIG. III-1. Diagram of the adsorption tube used in the gravimetric measurements of metal dispersion.

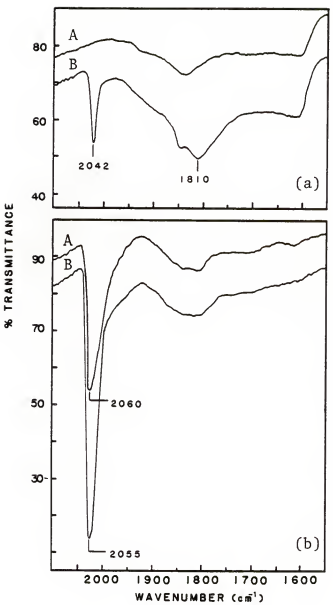

FIG. III-2. Infrared spectra of (a) 0.6% Pt·Wy. montmorillonite: (A) evacuated and (B) addition of 35 Torr CO; and (b) 3.0% Pt·Wy.montmorillonite: (A) addition of 35 Torr CO and (B) addition of 35 Torr CO for 1 hour and evacuated to 1 x 10^{-5} Torr.

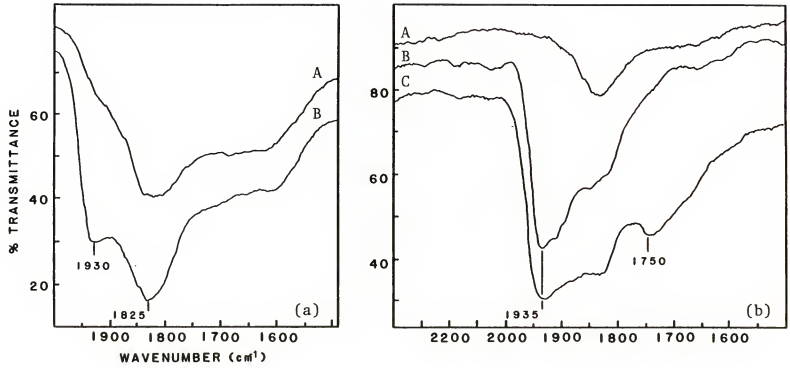

FIG. III-3. Infrared spectra of (a) 0.6% Pd·Wy.montmorillonite: (A) evacuated, (B) addition of 35 Torr CO; and (b) 3.0% Pd·Wy. montmorillonite: (A) evacuated, (B) addition of 35 Torr CO, and (C) evacuation of (B) to 1 x 10^{-5} Torr.

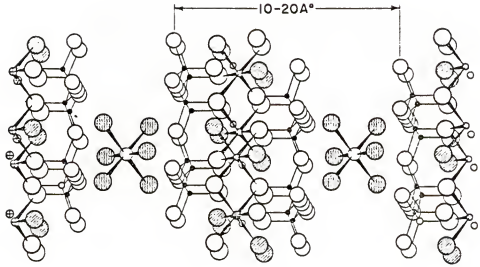

FIG. III-4. The structure of a smectite mineral illustrating the two tetrahedral silica sheets linked to the central octahedral sheet through oxygen apices. Shaded circles in the octahedral sheet represent hydroxyl groups bridge-bonded to adjacent structural cations. Hydrated cations are seen positioned between stacked smectite layers.

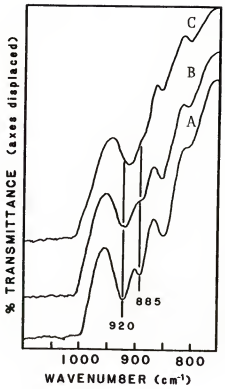

FIG. III-5. Infrared spectra of montmorillonite deformation bands recorded at various times during a hydrogen titration experiment: (A) 0 hrs., (B) 6 hrs., (C) 12 hrs.

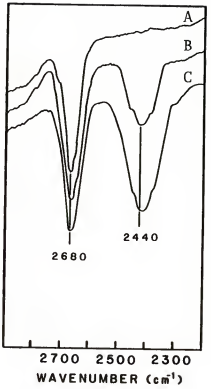

FIG. III-6. Infrared spectra showing the formation and increase in the ν(N-D) fundamental with time during a deuterium titration experiment: (A) 0 hrs., (B) 6 hrs., (C) 12 hrs.

CHAPTER IV
CONDENSED PHASE HYDROGENATION OF 1-HEXENE BY Pd AND Pt MONTMORILLONITE SUPPORTED CATALYSTS

Introduction

Differences in specific catalytic activity for supported metals have been explained in terms of metal crystallite and support effects. The metal crystallite effect originates with the arrangement of metal atoms on the surface of the crystallite, thereby determining the number and type of exposed faces. However, there is considerable evidence suggesting that this effect becomes influential only during certain types of reactions. Boudart et al. (38) have labelled these as demanding reactions in which multiple bond formation occurs and/or the reaction proceeds via several possible pathways. Several investigations (reviewed in Ref. 39) have documented increases in specific catalytic activity with the use of zeolites, in place of alumina or silica gels, as support matrices. This effect apparently arises by a modification of the electronic properties of small metal particles by the zeolite support. Dalla Betta and Boudart (40) and later Chukin et al. (41) proposed that sulfur resistance during isomerization and cracking reactions was a manifestation of the metal interaction with electron acceptor sites on the zeolite support

matrix. Naccache et al. (42) found that the rate of cyclopropane hydrogenation at room temperature is 100 times faster on PtNaY zeolite than Pt on SiO_2 or Al_2O_3. In fact, the presence of trivalent cations was found to further enhance the reaction rate. This was interpreted as an electrostatic field effect created by the support and/or cations which destabilized the cyclopropane ring.

The application of naturally occurring clay minerals as support matrices for noble metal catalyzed reactions has received little attention since the introduction of synthetic layered alumino-silicates in the early 1970s. A priori, montmorillonites would appear to be well-suited as support materials because of their high internal surface area, high cation exchange capacity, and high surface acidity. In Chapter II, we evaluated metal location, size distribution, and mean particle diameter for four loadings of palladium on a Wyoming (Wy.) montmorillonite. Our investigations demonstrated that for low metal loadings, very small particle diameters were obtainable in a narrow size distribution with little or no pretreatment prior to reduction. It was suggested that the high metal dispersions attained at low metal concentrations coupled with the unique suspension stability of the mineral in liquids make these catalysts a reasonable choice for condensed phase hydrogenations. This investigation was initiated to evaluate the catalytic activity of palladium supported on Wy. montmorillonite for the hydrogenation of 1-hexene in an ethanolic suspension. Particular

attention was focused on the influence of the montmorillonite support on catalytic activity and factors contributing to it.

Experimental

The preparation of palladium loaded Wy. montmorillonites, as well as the full characterization of mean particle diameters and the corresponding size distributions, was presented in Chapter II.

Reagents used in hydrogenation reactions were obtained in the purest grade available and used without further treatment. Hydrogen, acquired from Airco Specialty Gasses in grade 5.5, was rated at 99.999% pure. 1-hexene (99%) was purchased from Aldrich Chemical Company and absolute ethyl alcohol (dehydrated) from U.S. Industrial Chemical Company.

Hydrogenation reactions were run in a constant pressure apparatus similar to that described by Vanderheuval (43). The system was composed of three main parts: a water-jacketed hydrogenation cell, a graduated buret, and an automatic levelling unit as shown in Fig. IV-1.

Typically, 5.00-20.00 mg catalyst and 5.00 ml absolute ethanol were added to the hydrogenation cell and stirred for 30 minutes under flowing H_2 prior to hexene addition. The remainder of the system, including the levelling reservoir, filled with ethanol, was purged with H_2 for at least 15 minutes. At time zero, 0.125 to 0.750 ml hexene was injected

through an air-tight septum. Buret readings were taken at 15 second intervals and monitored until 25 ml H_2 was consumed. All reactions were run at 24°C. Rate constants were evaluated by assuming zero-order kinetics and using a least squares estimate of the slope. A minimum of six runs was used for determining the rate constant at each catalyst loading with the means and standard deviations given in Table IV-1.

As a control sample, a 5.0% Pd·Al_2O_3 catalyst was used as received from Alfa Chemical Company. Direct examination of the catalysts by transmission electron microscopy (TEM) showed an average crystallite diameter of 20Å with 90% of the sample population less than 30Å. Hydrogenation rate constants for this material are shown in Table IV-1.

Results

Rate constants for each catalyst loading, as deduced from a minimum of six hydrogenations of 1-hexene, are shown with their respective standard deviations (σ) in Table IV-1. It should be pointed out that for the six or more replications run at each loading, the quantity of catalyst added to the reaction vessel varied from 5.00 to 20.00 mg and the volume of hexene injected at the beginning of a run varied from 0.125 to 0.750 ml. Therefore, in the cases where the magnitude of σ approaches 30% of the average rate constant, an apparent retardation effect on reaction rates occurred, where the diffusion of the reactants to catalyst surfaces became the limiting

factor. Nonetheless, the variation in $\bar{k}m$ with catalyst metal weight demonstrates the effect of decreasing palladium dispersion and surface area.

Metal surface areas shown in Table IV-1 were determined from TEM particle diameter measurements. The transformation from particle diameter ($\bar{d}$) to metal surface area was calculated by using the relationship between particle size and dispersion proposed by Aben (44): $\bar{d} = 10 \times 0.885/(\text{dispersion})$; and the equation of Taylor et al. (45) for surface area as a function of dispersion: $S(m^2/gm\ \text{metal}) = (N\alpha/M) \times (\text{dispersion})$. In the latter equation, N is Avogadro's number, α is the cross-sectional area of a palladium atom (8.9Å), and M is the molecular weight of palladium.

For a valid comparison of catalytic activity between different metal loading, rate constants were also expressed in Table IV-1 in terms of the number of exposed surface atoms by dividing each $\bar{k}m$ by the metal surface area at that loading. These rate coefficients will be referred to as specific activities (ks). Unexpectedly, we found an increase in specific activity, beyond experimental error, with increasing metal content and decreasing surface area. However, Poltorak and Boronin (46) have found a similar effect for the hydrogenation of 1-hexene by Pt/SiO_2 samples of differing metal content and dispersion. They attributed this effect to structural changes in metal associated with variations in metal dispersion.

Preliminary experiments using a NH_4^+·Wyoming montmorillonite demonstrated that neither the support nor the reaction apparatus had any detectable catalytic activity. In addition, GC analysis of the reaction products confirmed that only hexane was formed during the hydrogenation of 1-hexene in ethanol.

Discussion

From the perspective of specific catalytic activity, the results of this study have established qualitative differences between Pd·Wy.montmorillonites which vary widely in metal dispersion and surface area. Indeed, at approximately equivalent metal contents, the 4.7% Pd·Wy.montmorillonite showed a specific activity that was nearly tenfold greater than the 5.0% $Pd \cdot Al_2O_3$ catalyst. Despite the findings of Poltorak and Boronin (46), the hydrogenation of 1-hexene should be insensitive to the nonuniformity of the metal surface. In fact, Cinneide and Clarke (47) have surveyed a number of structure-sensitivity studies and concluded that in most hydrogenation reactions, specific activity was independent of crystallite size. Clearly then, our observed variation in specific activity with crystallite size and the tenfold difference in specific activity between 4.7% Pd·Wy.montmorillonite and the 5.0% $Pd \cdot Al_2O_3$ must reflect the presence of a metal-support interaction.

A number of kinetic studies (45, 48, 49) have provided sufficient evidence to confirm the phenomenon of hydrogen

spillover from metal surfaces to acceptor sites on the support phase. In Chapter III we unequivocally established the role of structural iron (III) in naturally occurring Wyoming montmorillonite as hydrogen atom acceptor sites during the hydrogen titration of chemisorbed oxygen. It would appear from our results in this study, that a similar effect was manifest during the hydrogenation of 1-hexene by palladium supported on the same montmorillonite matrix. Under these circumstances, km, the rate constant expressed in terms of metal weight, represents the reaction rate at the metal surface plus a rate enhancement factor from hydrogen spillover. Assuming this spillover factor is constant throughout all metal loadings [we found a constant contribution in titration experiments which was independent of metal or metal loadings], then its influence on specific activity calculations should increase as the number of surface metal sites decreases. This produces higher specific activities at high loadings. If real, this effect has inflated all of our activity measurements to some extent and produced the apparent dichotomy of increasing specific activity with decreasing metal surface area. Unfortunately, the evidence at this point is circumstantial, yet the concept of reaction rate enhancement by the spillover of hydrogen atoms to the support is consistent with the results presented here and in earlier Chapters. Although the possibility of an electronic modification of the palladium metal by the support cannot be ruled out, this effect should reach a maximum at the smallest crystallite

diameter, thereby producing an increase in specific activity with decreasing particle size--a trend contrary to what we observed.

Conclusions

This study has demonstrated that palladium crystallites supported on Wy. montmorillonite are catalytically active toward the hydrogenation of 1-hexene. Indeed, the specific activity observed for these materials was nearly tenfold higher than a highly dispersed 5.0% $Pd \cdot Al_2O_3$ catalyst. We have postulated that this difference, coupled with the observation of increasing specific activity with decreasing metal surface area, was an artifact of hydrogen spillover from the metal to the support phase.

TABLE IV-1
RATE CONSTANTS FOR WY. MONTMORILLONITE SUPPORTED Pd CATALYSTS

Catalyst	$\overline{k}_m$ ($mol \cdot atm^{-1} \cdot s^{-1} \cdot g^{-1}_{Pd}$)	Standard Deviation (σ)	Surface Area (m^2/gm_{Pd})	k_a ($mol \cdot atm^{-1} \cdot s^{-1} \cdot m^{-2}$)
0.6% Pd·Wy.montmorillonite	1.79×10^{-2}	2.76×10^{-3}	196.5	9.11×10^{-5}
1.0% Pd·Wy.montmorillonite	1.56×10^{-2}	2.60×10^{-3}	110.8	1.41×10^{-4}
3.0% Pd·Wy.montmorillonite	7.60×10^{-3}	1.11×10^{-3}	50.4	1.50×10^{-4}
4.7% Pd·Wy.montmorillonite	4.68×10^{-3}	1.53×10^{-3}	25.2	1.86×10^{-4}
5.0% Pd·Al_2O_3	3.72×10^{-3}	1.02×10^{-3}	277.1	1.34×10^{-5}

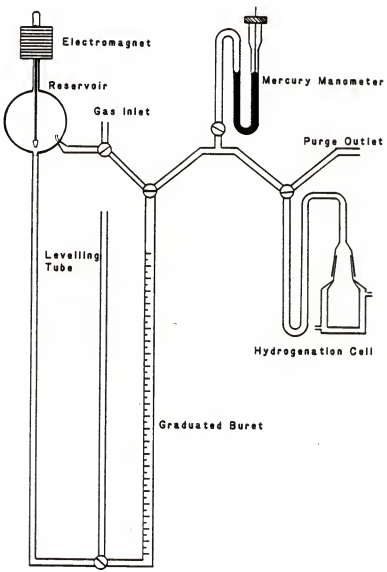

FIG. IV-1. Diagram of the constant pressure hydrogenation apparatus. A decrease in pressure, produced by hydrogen consumption, results in a contact break in the mercury manometer. This activates the electromagnet, lifting the reservoir plunger, allowing the flow of liquid until pressure is restored.

REFERENCES

1. Mortland, M.M., and Pinnavaia, T.J., *Nature (London), Phys. Sci.* 229, 75 (1971).

2. Pinnavaia, T.J., and Mortland, M.M., *J. Phys. Chem.* 75, 3957 (1971).

3. Pinnavaia, T.J., Hall, P.L., Cady, S.S., and Mortland, M.M., *J. Phys. Chem.* 78, 994 (1974).

4. Berkheiser, V.E., and Mortland, M.M., *Clays Clay Min.* 25, 105 (1977).

5. Berkheiser, V.E., and Mortland, M.M., *Clays Clay Min.* 26, (1978).

6. Krenske, D., Abdo, A., Van Damme, H., Cruz, M., and Fripiat, J.J., *J. Phys. Chem.* 84, 2447 (1980).

7. Pinnavaia, T.J., and Welty, P.K., *J. Am. Chem. Soc.* 97, 3819 (1975).

8. Rozenson, I., and Heller-Kalli, L., *Clays Clay Min.* 24, 271 (1976).

9. Primet, M., Bassert, S.M., Garbowski, E., and Mathieu, M.V., *J. Am. Chem. Soc.* 97, 3655 (1975).

10. Farmer, V.C., in "Infrared Spectra of Minerals," Chap. 15, Monograph 4, Mineralogical Society, London, 1974.

11. Hiraishi, J., Nakagawa, I., and Shimanovchi, T., *Spectrochim. Acta* 24A, 819 (1968).

12. Poulet, H., Delorme, P., and Mathiev, J.P., *Spectrochim. Acta* 20, 1855 (1964).

13. Nakamoto, K., in "Infrared and Raman Spectra of Inorganic and Coordination Compounds," 3rd Ed. John Wiley & Sons, New York, 1978, p. 199.

14. Rozenson, I., and Heller-Kalli, L., *Clays Clay Min.* 24, 283 (1976).

15. Stucki, J.W., Roth, C.B., Baitinger, W.E., *Clays Clay Min.* 24, 289 (1976).

16. Clementz, D.M., Pinnavaia, T.J., and Mortland, M.M., *J. Phys. Chem.* 77, 196 (1973).

17. Burba, III, J.L., and McAtee, Jr., J.L., *Clays Clay Min.* 25, 113 (1977).

18. Swift, H.E., in "Advanced Materials in Catalysis," Chap. 7, Academic Press, New York, 1977.

19. Granquist, W.T., U.S. Patent 3,252,757 (1966).

20. Csicsery, S.M., U.S. Patents 3,617,488; 3,617,489; 3,617,490; 3,617,491 (1971).

21. Csicsery, S.M., and Kittrell, J.R., U.S. Patent 3,632,500 (1972).

22. Jaffe, J., U.S. Patents 3,652,457; 3,664,971; 3,664,972; 3,664,973 (1972).

23. Jaffe, J., and Kittrell, J.R., U.S. Patent 3,671,425 (1972).

24. Kittrell, J.R., U.S. Patents 3,632,501; 3,632,502 (1972).

25. Malaskey, B.F., U.S. Patent 3,682,811 (1972).

26. Schmidt, K.H., and Müller, A., *J. Mol. Struct.* 22, 343 (1974).

27. Hendra, P.J., *Spectrochim. Acta* 23A, 1275 (1967).

28. Benson, J.E., and Boudart, M., *J. Catal.* 4, 704 (1965).

29. Mears, D.E., and Hansford, R.C., *J. Catal.* 9, 125 (1967).

30. Wilson, G.R., and Hall, W.K., *J. Catal.* 17, 190 (1970).

31. Kikuchi, E., Flynn, P.C., and Wanke, S.E., *J. Catal.* 34, 132 (1974).

32. Sermon, P.A., and Bond, G.C., *Catal. Rev.* 8(2), 211 (1973).

33. Berkheiser, V.E., Rao, P.V., and Pothier, W.G., *Rev. Sci. Instrum.* 52(1), 101 (1981).

34. Sheppard, N., and Nguyen, T.T., "Advances in Infrared and Raman Spectroscopy," Vol. 5 83, Heyden and Sons Ltd., London, 1978.

35. Boudart, M., *Advan. Catal.* 20, 153 (1969).

36. Benson, J.E., Kohn, H.W., and Boudart, M., *J. Catal.* 5, 307 (1966).

37. Popova, N.M., and Sokol'skii, D.V., *Tr. Inst. Org. Katal. Electro. Acad. Navk. Kaz. SSR* 1, 3 (1971).

38. Boudart, M., Aldag, A., Benson, J.E., Dougharty, A., and Harkins, C.G., *J. Catal.* 6, 92 (1966).

39. Gallezot, P., *Catal. Rev.-Sci. Eng.* 20(1), 141 (1979).

40. Dalla Betta, R.A., and Boudart, M., *Proc. Int. Congr. Catal. 5th,* 1329 (1973).

41. Chukin, G.D., Landau, M.V., Kruglikov, V., Agrievskii, D.A., Smirnov, B.V., Belozerov, A.L., Asrieva, V.D., Goncharova, N.V., Radchenko, E.D., Konovalcherov, O.D., and Agafonoy, A.V., *Proc. Int. Congr. Catal. 6th,* 668 (1977).

42. Naccache, C., Kaufherr, N., Dufaux, M., Pandiera, J., and Imelik, B., in "Molecular Sieves-II," American Chemical Society, Washington, D.C., 1977, p. 538.

43. Vanderheuval, F.A., *Anal. Chem.* 24, 847 (1952).

44. Aben, P.C., *J. Catal.* 10, 224 (1968).

45. Taylor, G.F., Thomson, S.J., and Webb, G., *J. Catal.* 8, 388 (1967).

46. Poltorak, O.M., and Boronin, V.S., *Russ. J. Phys. Chem.* 40, 1436 (1966).

47. Cinneide, A.D.O., and Clarke, J.K.A., *Catal. Rev.* 7, 213 (1972).

48. Carter, J.L., Lucchesi, P.J., Sinfelt, J.H., and Yates, D.J.C., *Proc. Int. Congr. Catal. 3rd,* 644 (1965).

49. Sinfelt, J.H., and Lucchesi, P.J., *J. Amer. Chem. Soc.* 85, 3365 (1963).

BIOGRAPHICAL SKETCH

Jeffrey Baker Harrison was born in Columbus, Ohio, on August 20, 1953, to Timothy A. and Laura Lee B. Harrison. Most of his early life was spent in this city where he finally completed his secondary education at The Columbus Academy, graduating in 1972. From there, he attended Centre College of Kentucky for two years and transferred to Purdue University where he completed his undergraduate studies and received a Bachelor of Science degree in 1977. The same year, he entered the University of Florida in pursuit of a Master of Science. With the subsequent birth of a son and an unfortunate divorce, he abandoned the MS program and petitioned the Graduate School to directly pursue a Doctor of Philosophy degree in soil mineralogy and chemistry.

Jeffrey will leave Gainesville in August, 1982, to enter the chemical industry as a research scientist.

I certify that I have read this study and that in my opinion it conforms to acceptable standards of scholarly presentation and is fully adequate, in scope and quality, as a dissertation for the degree of Doctor of Philosophy.

Bob G. Volk, Chairman
Associate Professor of Soil Science

I certify that I have read this study and that in my opinion it conforms to acceptable standards of scholarly presentation and is fully adequate, in scope and quality, as a dissertation for the degree of Doctor of Philosophy.

Vaughn E. Berkheiser, Cochairman
Assistant Professor of Soil Science

I certify that I have read this study and that in my opinion it conforms to acceptable standards of scholarly presentation and is fully adequate, in scope and quality, as a dissertation for the degree of Doctor of Philosophy.

Wallace S. Brey
Professor of Chemistry

I certify that I have read this study and that in my opinion it conforms to acceptable standards of scholarly presentation and is fully adequate, in scope and quality, as a dissertation for the degree of Doctor of Philosophy.

Jimmy J. Street
Assistant Professor of Soil Science

This dissertation was submitted to the Graduate Faculty of the College of Agriculture and to the Graduate Council, and was accepted as partial fulfillment of the requirements for the degree of Doctor of Philosophy.

May 1982

Jack L. Fry

Dean, College of Agriculture

Dean for Graduate Studies and Research